

Noise-Induced Transitions in a Barotropic β -Plane Channel

PHILIP SUR A*

Meteorologisches Institut der Universität Hamburg, Hamburg, Germany

(Manuscript received 27 February 2001, in final form 15 May 2001)

ABSTRACT

The concepts of multiplicative stochastic perturbations and noise-induced transitions are applied to a quasi-geostrophic β -plane model of barotropic flow over topography. The spectral three-component low-order representation of this configuration yields the Charney–DeVore (CDV) model. The externally prescribed damping of the system is allowed to scatter around a mean value. The stochastic representation of the damping term leads to a multiplicative stochastic forcing. The Fokker–Planck equation and the stochastic differential equation of the low-order CDV model are solved numerically. It is found that the qualitative behavior of the system is a function of the multiplicative noise level. In particular, the effect of multiplicative noise is not simply a smoothing of the probability density function, as it would be for pure additive noise. Rather, multiplicative noise leads to the high-index state being favored over the low-index state. The concept of noise-induced transitions explains this behavior. The noise-induced transition of the stochastic low-order model is confirmed by numerical integrations of a corresponding gridpoint model with many more degrees of freedom than the spectral model. It is suggested that the statistics of the unresolved physical processes could be an important factor in understanding the behavior of midlatitude large-scale atmospheric dynamics.

1. Introduction

It has long been observed that the atmospheric midlatitude circulation appears to alternate between a zonal high-index flow and a low-index flow with a pronounced wave component (e.g., Pandolfo 1993). This behavior suggests that there may exist more than one large-scale flow regime consistent with a given external forcing. Regimes are defined as regions in the system's phase space where the probability of occurrence attains local maxima. The definition is due to the fact that a chaotic system may possess a set of attractor basins each much smaller than the phase space of the entire system. Charney and DeVore (1979) (CDV) were the first who proposed that the occurrence of large-scale flow regimes may be due to multiple equilibria of the nonlinear governing equations. They suggest that blocking and zonal flow could be associated with two stable stationary solutions of the spectrally truncated nonlinear barotropic quasigeostrophic vorticity equation. Within this framework Legras and Ghil (1985) elucidate the dynamical importance of unstable fix points. Steady states that are

unstable to a small number of modes, but stable to a large number of modes, may act to steer a time-dependent model, thus providing a mechanism for a temporarily persistent regime. Nevertheless, the observational evidence for multiple states or regimes in the atmospheric circulation is rather sparse. Furthermore, the relevance of multiple equilibria in truncated models has been questioned by Tung and Rosenthal (1985).

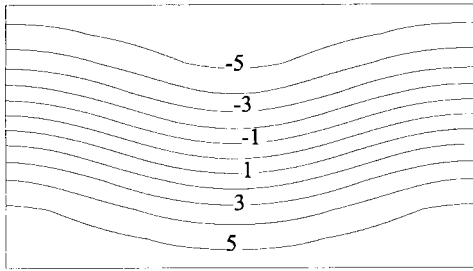
One fundamental drawback of the low-order CDV model is that the trajectories of the system always move toward one of the two stable steady states. That is, the deterministic CDV model is not able to explain transitions between the equilibria. To overcome this problem, transitions between the two regimes might occur as a result of high-frequency fluctuations not resolved in the three-component low-order system. In particular, these unresolved fluctuations are often parameterized by additive stochastic processes. A stochastic representation of the truncated high-frequency modes has been applied to the CDV model by Egger (1981), Benzi et al. (1984), and DeSwart and Grasman (1987). The additive noise forces the system to alternately visit the attracting domains of the two stable equilibria. Thus, the system shows a bimodal behavior. Even the neighborhood of the unstable equilibrium is visited for some time during the transition between the two stable equilibria. This supports the conjecture of Legras and Ghil (1985) that unstable equilibria are important for atmospheric dynamics.

In climate models the stochastic forcing is normally

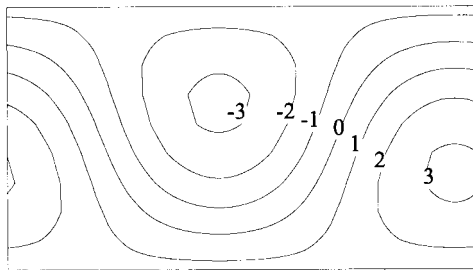
* Current affiliation: Scripps Institution of Oceanography, University of California, San Diego, La Jolla, California.

Corresponding author address: Dr. Philip Sura, Scripps Institution of Oceanography, University of California, San Diego, 9500 Gilman Drive, La Jolla, CA 92093-0230.
E-mail: pgsura@ucsd.edu

Equilibrium 1 (stable)



Equilibrium 2 (unstable)



Equilibrium 3 (stable)

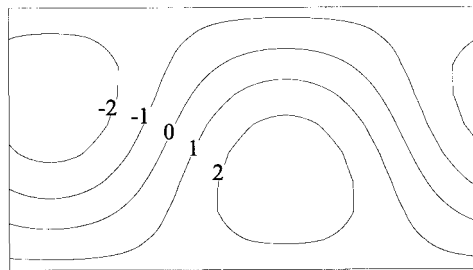


FIG. 1. Nondimensional streamfunction patterns for the equilibria of the deterministic CDV model ($a = 1$, $b = 1$, $C = 0.2$, $x_1^* = 4.19$, $\beta = 2.55$).

introduced as an additive process. That is, the intensity of the the stochastic forcing is treated to be independent of the state of the system. However, the stochastic forcing may also represent the fluctuations of model parameters. In that case, the stochastic process appears as multiplicative noise. It is well-known that multiplicative noise can substantially change the dynamical behavior of nonlinear systems (Horsthemke and Lefever 1984; Landa and McClintock 2000). An example is a phenomenon that is called a “noise-induced transition” (Horsthemke and Lefever 1984). Noise-induced transitions can occur if a certain amount of multiplicative noise is present in the system under consideration. Then, the system can undergo a characteristic qualitative

TABLE 1. Dimensional model parameters.

Coriolis parameter	$f_0 = 1.0 \times 10^{-4} \text{ s}^{-1}$
Beta effect	$\beta = 1.6 \times 10^{-11} \text{ m}^{-1} \text{ s}^{-1}$
Layer depth	$H = 1 \times 10^4 \text{ m}$
Ekman layer depth	$D_E = 120 \text{ m}$
Acceleration of gravity	$g = 9.81 \text{ m s}^{-2}$
Topography amplitude	$h_0 = 500 \text{ m}$
Forcing amplitude	$\psi_0^* = 6.7 \times 10^6 \text{ m}^2 \text{ s}^{-1}$
Domain extent (east–west)	$L_x = 3 \times 10^6 \text{ m}$
Domain extent (north–south)	$L_y = 1.5 \times 10^6 \text{ m}$

change of its probability density function due to the impact of the external multiplicative noise.

The relevance of using multiplicative noise in atmospheric models is twofold. On the one hand, it will be impossible in the foreseeable future to perform long-term integrations of complex high-resolution atmospheric models in order to resolve decadal or even centennial timescales. At present simplified deterministic atmospheric models are often used to explore low-frequency climate variability (e.g., Kurgansky et al. 1996; Dethloff et al. 1998). In general, there is a crucial interest in modeling the low-frequency behavior of the atmospheric circulation (Corti et al. 1999). Thus, there is a potential need for more sophisticated stochastic models beyond linear Langevin equations to understand long-term climate variability. Majda et al. (1999) show, using the same model of barotropic quasigeostrophic flow over topography as in the present paper, that the effect of the original 57 degrees of freedom can be well represented by a theoretically predicted stochastic model with only 3 degrees of freedom. They use a sophisticated stochastic approach, including multiplicative noise. On the other hand, most atmospheric models, simplified or even complex, parameterize unresolved processes using deterministic approximations. Sardeshmukh et al. (2001) show how deterministic parameterization of actually highly variable processes in numerical prediction models contribute to climatological mean errors found in those models. Therefore, there is a need to understand the basic effects of multiplicative noise in atmospheric models.

In the present study the concepts of multiplicative stochastic perturbations and noise-induced transitions are applied to a quasigeostrophic β -plane model of barotropic flow over topography. The spectral three-component low-order representation of this configuration yields the CDV model. The externally prescribed damping parameter of the system scatters around a mean value. Therefore, the stochastic representation of the damping term leads to a multiplicative stochastic forcing term. Both the low-order CDV model and the corresponding gridpoint model with many more degrees of freedom are investigated in the multiplicative stochastic framework. In particular, one intention is to investigate the stochastic dynamics of the CDV model with multiplicative noise. In addition, the relationship to the equivalent stochastically perturbed high-order gridpoint

model is studied. This is done to investigate if the effect of multiplicative noise in the low-order environment is also present in the corresponding high-order gridpoint model. In this framework it is important to note that Charney and DeVore (1979) and Yoden (1985b) show that the existence of multiple equilibria is not an artifact of the low-order model. Indeed, the corresponding gridpoint model with many more degrees of freedom shows the two stable equilibria, too. Nevertheless, a priori it is not obvious if noise-induced transitions, which are normally observed in systems with very few degrees of freedom, can also be observed in the high-order system.

In section 2 the quasigeostrophic channel model and its low-order spectral representation, the CDV model, is described briefly. Moreover, the stochastically perturbed CDV model and the corresponding Fokker–Planck equation is introduced. Section 3 presents the experimental design and the results of the numerical experiments. Finally, section 4 provides a discussion of the results.

2. The model

a. Quasigeostrophic equation

In this paper we confine our study to the behavior of a simple barotropic quasigeostrophic flow of undisturbed height H over topography with a bottom elevation $h(x, y)$ in a midlatitude β -plane channel. The governing equation reads

$$\begin{aligned} \frac{\partial}{\partial t}(\nabla^2\psi - \gamma^2\psi) + J\left(\psi, \nabla^2\psi + f_0\frac{h}{H} + \beta y\right) \\ = -f_0\frac{D_E}{2H}\nabla^2(\psi - \psi^*), \end{aligned} \quad (1)$$

where $\psi(x, y, t)$ is the streamfunction, $J(a, b) = \partial a/\partial x \partial b/\partial y - \partial a/\partial y \partial b/\partial x$ the Jacobian operator, and $\gamma^2 = f_0^2/gH$ the squared inverse Rossby radius (g is the acceleration of gravity and f_0 is the Coriolis parameter). The right-hand side of (1) contains the effect of a frictionally induced vorticity sink and a parameterized vorticity source. The parameter ψ^* is a forcing streamfunction that parameterizes the meridional temperature gradient. In the classical deterministic model the forcing and dissipation terms are proportional to the depth of the bottom Ekman layer $D_E = (2A_v/f_0)^{1/2}$, where A_v is the vertical turbulent viscosity coefficient. Thus, $\tau = 2H/f_0D_E = 2/(f_0E_v^{1/2})$, with the vertical Ekman number $E_v = (2A_v)/(f_0H^2)$, is a characteristic damping timescale for the decay of the quasigeostrophic motion under the influence of Ekman layer friction. A derivation of the equations can be found in Pedlosky (1987).

If the motion is considered in a channel of width $0 \leq y \leq L_y$, and length $0 \leq x \leq L_x$, the boundary condition of no normal transport at the channel boundaries requires ψ to be constant at $y = 0$ and $y = L_y$. In addition, the ageostrophic boundary condition requires $\int_0^{L_x} \partial\psi/\partial y$

$dx = 0$ at $y = 0$ and $y = L_y$ as well. Furthermore, periodic boundary conditions are used: $\psi(x, y, t) = \psi(x + L_x, y, t)$.

In the entire study the bottom topography $h(x, y)$ and the forcing streamfunction ψ^* are assumed to have simple sinusoidal structures with amplitudes h_0 and ψ_0^* to model a ridge–trough topography and a meridional temperature gradient:

$$\begin{aligned} h(x, y) &= h_0 \cos\left(\frac{2\pi x}{L_x}\right) \sin\left(\frac{\pi y}{L_y}\right), \\ \psi^* &= \psi_0^* \cos\left(\frac{\pi y}{L_y}\right). \end{aligned} \quad (2)$$

If not stated otherwise, the dimensional model parameters used for the subsequent experiments have values summarized in Table 1. These are the values used in the study of DeSwart and Grasman (1987).

b. Low-order model

A spectral model of (1) and (2) can be derived by expanding ψ , ψ^* , and h in orthonormal eigenfunctions of the Laplace operator. The low-order model studied in this paper only retains three modes. The nondimensional three-component model equations of the barotropic quasigeostrophic flow over topography driven by an external streamfunction forcing read (see appendix)

$$\begin{aligned} \dot{x}_1 &= bx_3 - C(x_1 - x_1^*) \\ \dot{x}_2 &= -ab\left(x_1 - \frac{1}{2}\beta\right)x_3 - Cx_2 \\ \dot{x}_3 &= ab\left(x_1 - \frac{1}{2}\beta\right)x_2 - \frac{1}{2}ax_1 - Cx_3. \end{aligned} \quad (3)$$

This set of equations is often designated as the CDV equations or model. It is well known that for a suitable range of parameters the unperturbed low-order system (3) exhibits three equilibria E_1 , E_2 , and E_3 (see Fig. 1). In the present study the nondimensional parameters are identical to DeSwart and Grasman (1987): $a = 1$, $b = 1$, $C = 0.2$, $x_1^* = 4.19$, $\beta = 2.55$. Equilibrium $E_1 = (3.91, 0.74, -0.06)$ consists of a nearly zonal high-index flow and is stable, $E_2 = (1.88, 1.40, -0.46)$ shows an intermediate flow and appears to be unstable. Equilibrium $E_3 = (0.94, -1.06, -0.65)$ shows a low-index flow with a pronounced wave component and is stable. For arbitrary initial conditions the phase space trajectories always tend to one of the two stable equilibria. A detailed discussion of the CDV model can be found, for example, in Charney and DeVore (1979), Egger (1981), Yoden (1985a), and DeSwart (1988). Moreover, Charney and DeVore (1979) and Yoden (1985b) show that the existence of multiple equilibria is not an artifact of the low-order model. Indeed, a gridpoint model with

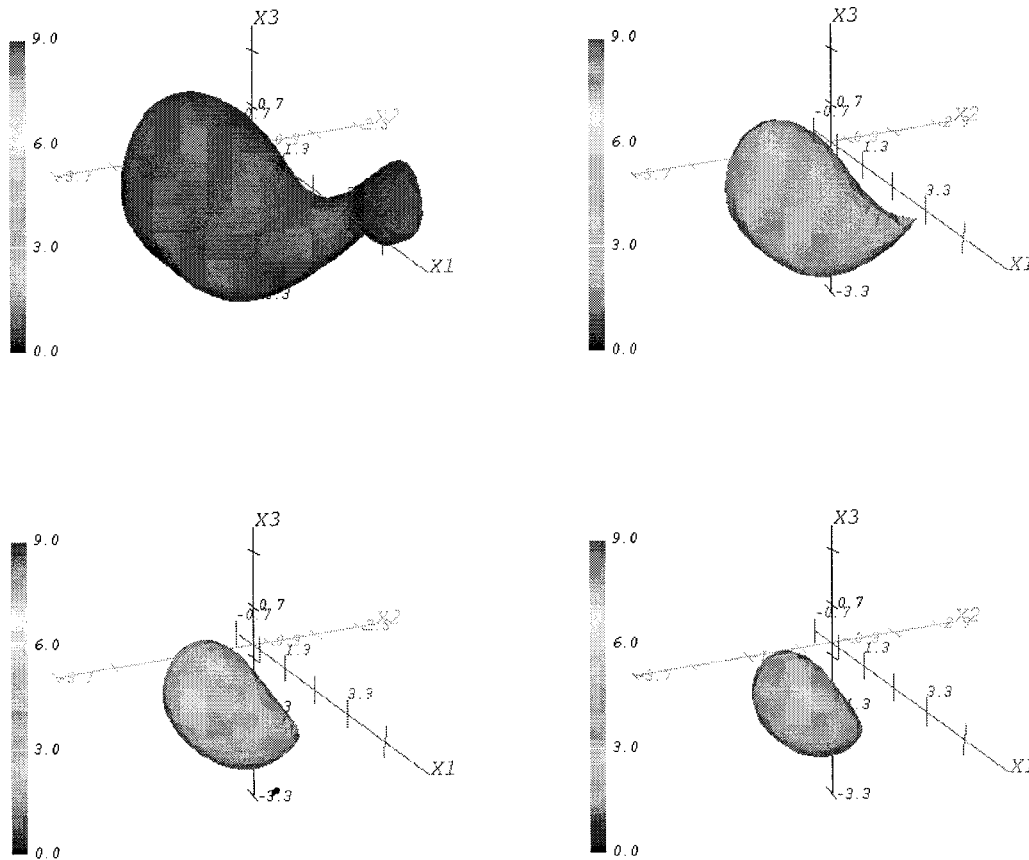


FIG. 2. Steady-state probability density isosurfaces of the CDV Fokker-Planck equation with multiplicative and additive noise: $\sigma_i^M = 0.1$ and $\sigma_i^A = 0.3$ ($i = 1, 2, 3$); $a = 1$, $b = 1$, $C = 0.2$, $x_1^* = 4.19$, $\beta = 2.55$. Isosurface values from upper left to lower right: 1.0, 2.0, 3.0, 4.0.

many more degrees of freedom than the spectral model shows two stable equilibria, too.

c. Stochastic perturbations of the CDV model and the corresponding Fokker-Planck equation

Because the undisturbed CDV model does not exhibit transitions between the stable equilibria the model is unrealistic. Transitions between the two regimes might occur as a result of fluctuations not resolved in undisturbed low-order system. For this reason it is assumed that the CDV model can be made more realistic by introducing stochastic perturbations. As argued by Egger (1981) there are at least two possibilities to introduce noise in the CDV model. On the one hand the modes retained in the CDV equations are perturbed by additive noise components. The additive stochastic components mimics the influence of the truncated modes; this possibility is investigated by Egger (1981). On the other hand, the external parameters of the model may fluctuate. That is, if the system resides near one of the stable equilibria, and if an external parameter changes to make this equilibrium unstable, the system may tend to another equilibrium (Egger 1981). For the CDV model it

seems to be meaningful to stochastically perturb the frictional parameter C to parameterize the mixing due to turbulent eddies. Deterministic models usually characterize this damping with a constant parameter. Thus, the stochastic differential equations (SDEs) corresponding to the CDV model are

$$\begin{aligned} \dot{x}_1 &= bx_3 - (C + \eta_1^M)(x_1 - x_1^*) + \eta_1^A \\ \dot{x}_2 &= -ab\left(x_1 - \frac{1}{2}\beta\right)x_3 - (C + \eta_2^M)x_2 + \eta_2^A \\ \dot{x}_3 &= ab\left(x_1 - \frac{1}{2}\beta\right)x_2 - \frac{1}{2}ax_1 - (C + \eta_3^M)x_3 + \eta_3^A, \end{aligned} \tag{4}$$

where η_i^A are the additive stochastic components. Note that the stochastic components η_i^M that perturb the frictional parameter C lead to a multiplicative stochastic forcing, except the forcing term $\eta_1^M x_1^*$, which is indeed an additive stochastic term. For convenience, the nomenclature of η_i^M as a multiplicative stochastic forcing is retained. In the subsequent discussion all stochastic components η_i^A and η_i^M are assumed to be independent

Gaussian white noise processes with corresponding amplitudes σ_i^A and σ_i^M :

$$\begin{aligned}\langle \eta_i^A(t) \rangle &= 0, & \langle \eta_i^A(t) \eta_i^A(t') \rangle &= (\sigma_i^A)^2 \delta(t - t') \\ \langle \eta_i^M(t) \rangle &= 0, & \langle \eta_i^M(t) \eta_i^M(t') \rangle &= (\sigma_i^M)^2 \delta(t - t'),\end{aligned}\quad (5)$$

where $\langle \dots \rangle$ denotes the averaging operator. Because of the Gaussian distribution of the noise it is possible that $C + \eta_i^M$ becomes negative occasionally. Despite the fact that the deterministically defined depth of the Ekman layer cannot become negative, this is not a conceptual problem because it is known that turbulent eddy fluxes can occasionally change their sign as well.

The probability density function of the SDE is governed by the corresponding Fokker–Planck equation. In general, if an n -dimensional SDE is written as

$$\frac{d\mathbf{x}}{dt} = \mathbf{A}(\mathbf{x}) + \mathbf{B}(\mathbf{x})\boldsymbol{\eta}^M + \boldsymbol{\eta}^A, \quad (6)$$

with the $n \times n$ matrix, \mathbf{B} , the corresponding Fokker–Planck equation for the probability density function $p(\mathbf{x}, t)$ reads (e.g., Gardiner 1985; Horsthemke and Lefever 1984)

$$\begin{aligned}\frac{\partial p(\mathbf{x}, t)}{\partial t} &= -\sum_i \frac{\partial}{\partial x_i} \left[A_i + \alpha \sum_{j,k} (\sigma_i^M)^2 \left(\frac{\partial}{\partial x_j} B_{ik} \right) B_{jk} \right] p(\mathbf{x}, t) \\ &+ \frac{1}{2} \sum_{i,j} (\sigma_i^M)^2 \frac{\partial^2}{\partial x_i \partial x_j} (\mathbf{B}\mathbf{B}^T)_{ij} p(\mathbf{x}, t) \\ &+ \frac{1}{2} \sum_i (\sigma_i^A)^2 \frac{\partial^2}{\partial x_i^2} p(\mathbf{x}, t),\end{aligned}\quad (7)$$

where α can have two different values, to yield two physically important stochastic calculi: the Itô ($\alpha = 0$) and the Stratonovich calculus ($\alpha = 1/2$). The Fokker–Planck equation describes the conservation of the probability density $p(\mathbf{x}, t)$ of the system described by the SDE (6). The first term in angular brackets describes the dynamics of the deterministic system and is called the deterministic drift. The second term in angular brackets, which does not occur in Itô systems ($\alpha = 0$), is called the noise-induced drift. The remaining terms cause the diffusion of the system. The first diffusive term is a consequence of the multiplicative noise and, thus, depends on the state of system. The second diffusive term is due to the additive noise and is independent of the state of the system. Note that for the particular case of the stochastic CDV model (4) no mixed derivatives appear in the corresponding CDV Fokker–Planck equation due to the simple structure of the matrix \mathbf{B} .

For a detailed discussion of stochastic integration and the differences between Itô and Stratonovich SDEs see, for example, Horsthemke and Lefever (1984) or Gardiner (1985). In briefly summarizing, the Stratonovich calculus resembles most directly the situation where rap-

idly fluctuating quantities with small but finite correlation times are parameterized as white noise. Thus, the Stratonovich calculus is preferred in the subsequent calculations. The Itô stochastic calculus is used where discrete uncorrelated fluctuations are approximated as continuous white noise.

3. Results

In this section numerical solutions of the CDV Fokker–Planck equation (7) in the Stratonovich interpretation ($\alpha = 1/2$) are presented and discussed. To verify and interpret the results of the Fokker–Planck equation numerical integrations of the stochastic CDV model (6) are performed as well. Moreover, stochastically perturbed integrations of the high-order gridpoint model (1) and (2) are qualitatively compared with the phenomenology of the stochastic low-order models.

a. Solutions of the CDV Fokker–Planck equation

Analytic solutions of the Fokker–Planck equation (7) can only be found for limited cases; for more general cases numerical methods must be used. In this paper the semi-implicit Chang–Cooper method is implemented to solve (7) (Chang and Cooper 1970; Park and Petrosian 1996). The Chang–Cooper method is a flux-conservative finite-difference scheme second order in time. It is originally designed to solve one-dimensional Fokker–Planck equations. Nevertheless, an extension of this method to multidimensional problems is straightforward using the operator splitting method (Park and Petrosian 1996; Press et al. 1992). A regular grid with a mesh size 0.1 and $100 \times 100 \times 100$ grid points is used. The domain of computation is chosen to be the cubic $[-2.5: 7.5, -5:5, -5:5]$ that encloses the fix points of the deterministic CDV model for the used parameter values. The nondimensional time step is set to 0.25 (0.96 days in dimensional units). The CDV Fokker–Planck equation is integrated until a steady state is reached, which is attained at least after 100 days of integration, in agreement with Egger (1981). The initial distribution of the probability density p is chosen to be a symmetric three-dimensional Gaussian, with std dev 2, centered in the origin of the system. Other initial distributions do not change the subsequent results. The value of the integrated probability density p is conserved and is arbitrarily set to 100.

The parameter varied is the strength of the multiplicative noise (σ_i^M). The strength of the additive noise (σ_i^A) and the amplitude of the forcing (x_1^*) remain unchanged for the reference experiments ($a = 1, b = 1, C = 0.2, x_1^* = 4.19, \beta = 2.55$). These reference experiments show the main results and are, therefore, presented and discussed in detail. For convenience the strength of the multiplicative and additive noise components are chosen to have the same values in each dimension: $\sigma_1^M = \sigma_2^M = \sigma_3^M$ and $\sigma_1^A = \sigma_2^A = \sigma_3^A$. The

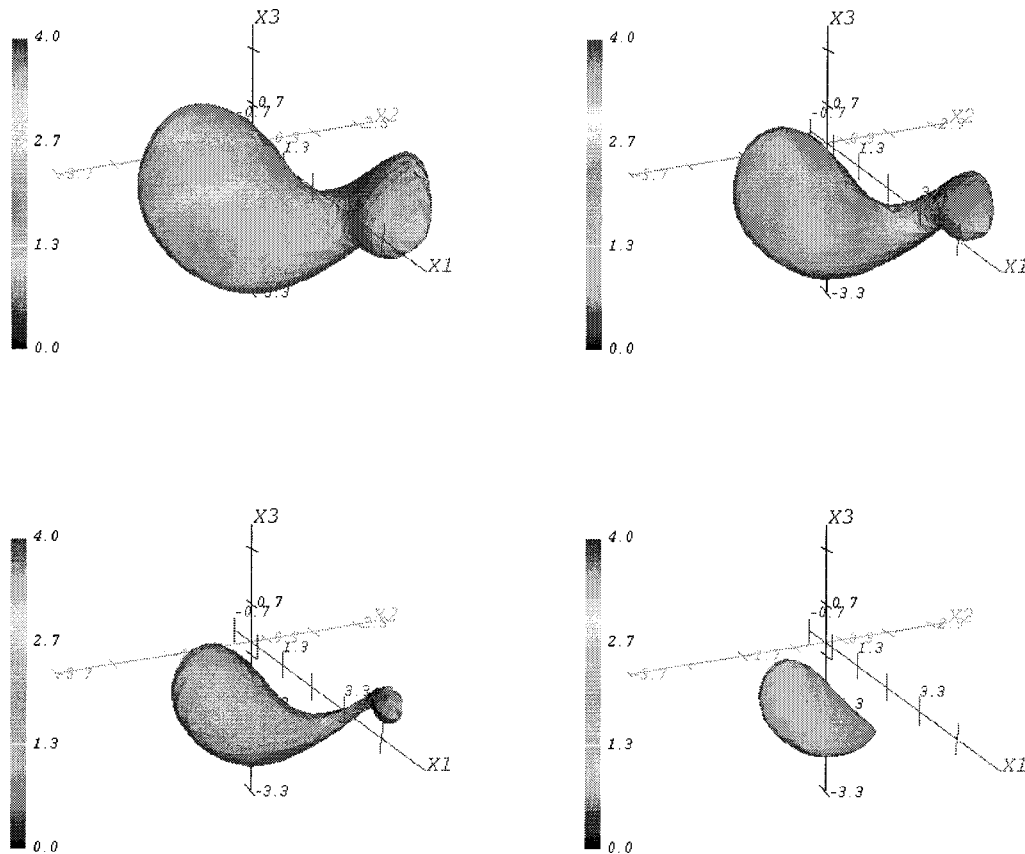


FIG. 3. Steady-state probability density isosurfaces of the CDV Fokker-Planck equation with multiplicative and additive noise $\sigma_i^M = 0.2$ and $\sigma_i^A = 0.3$ ($i = 1, 2, 3$); $a = 1$, $b = 1$, $C = 0.2$, $x_1^* = 4.19$, $\beta = 2.55$. Isosurface values from upper left to lower right: 1.0, 1.5, 2.0, 2.5.

strength of the additive noise is set to $\sigma_i^A = 0.3$. In the following the steady-state solutions of the CDV Fokker-Planck equation are presented as three-dimensional isosurfaces. An isosurface is the three-dimensional extension of the familiar two-dimensional isoline. The difference is that one two-dimensional isoline plot with several isolines is enough to present the structure of a two-dimensional field. In contrast several three-dimensional plots with only one isosurface each are necessary to present the general structure of a three-dimensional field. Note that, as in the two-dimensional case, the choice of the shown isosurfaces depends on the structure of the three-dimensional field. For each set of parameters four different valued isosurfaces are presented to qualitatively reveal the three-dimensional structure of the probability density function. Figures 2, 3, 4, and 5 display the steady-state probability density for four different multiplicative noise levels $\sigma_i^M = 0.1, 0.2, 0.3$, and 0.4 .

With $\sigma_i^M = 0.1$ (Fig. 2) the system shows a nearly monomodal low-index behavior. The most probable states are clustered around the low-index equilibrium E_3 . Only the 1.0 isosurface shows a remainder of the high-index equilibrium E_1 . Nevertheless, the dominant

maximum values of the probability density, up to 9.0, are centered inside the 4.0 isosurface near the low-index flow E_3 . Enhancing the multiplicative noise level to $\sigma_i^M = 0.2$ (Fig. 3), the system begins to show a weak bimodality. However, the maximum values of the probability density, up to 4.0, are centered inside the 2.5 isosurface near the low-index equilibrium E_3 . With $\sigma_i^M = 0.3$ (Fig. 4) the system shows a more pronounced bimodal behavior. The most probable states, with maximum probability densities up to 2.6, are now near the zonal high-index equilibrium E_1 . Nevertheless, the low-index states near the equilibrium E_3 have only a slightly lower probability. Thus, the system shows a clear bimodal behavior. Further enhancement of the multiplicative noise level to $\sigma_i^M = 0.4$ (Fig. 5) gives rise to a nearly monomodal high-index flow. The most probable states, with maximum probability densities up to 2.9, have entirely moved to the neighborhood of the high-index equilibrium E_1 . Only the 0.75 isosurface shows a remainder of the low-index equilibrium E_3 . The dominant maximum values of the probability density are centered inside the 2.25 isosurface in the neighborhood of the zonal high-index equilibrium E_1 .

In summarizing, one observes that the qualitative

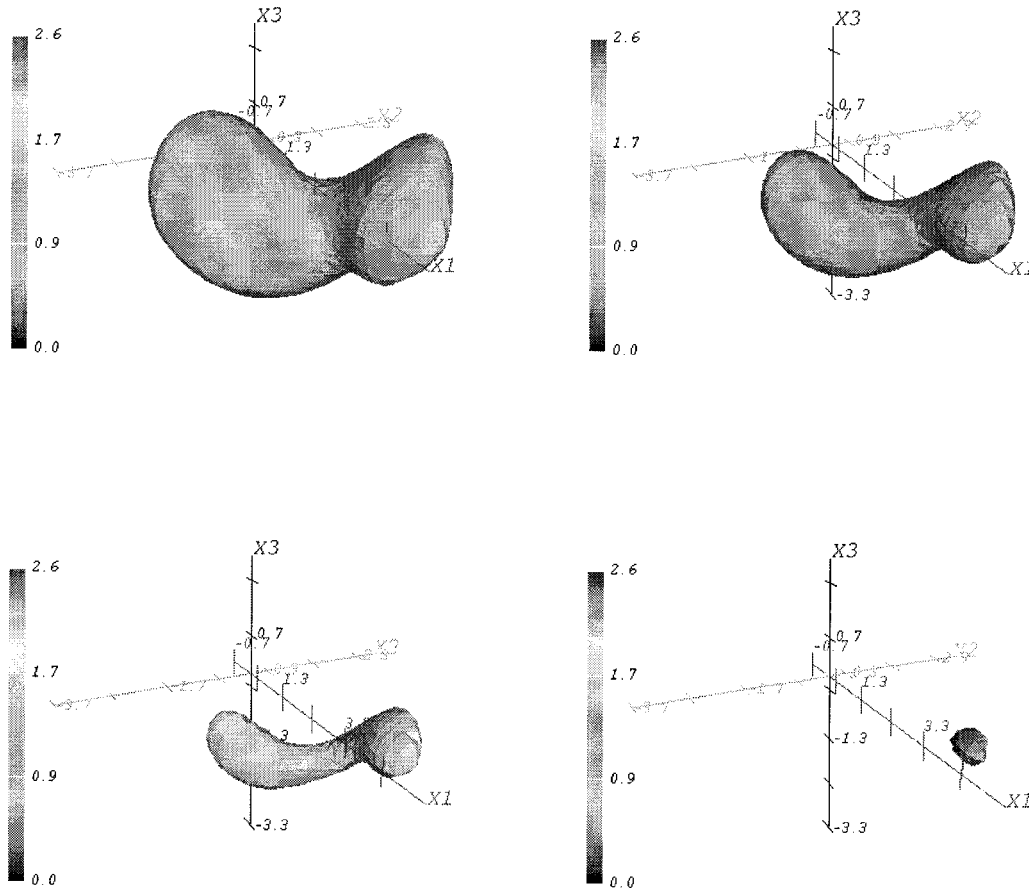


FIG. 4. Steady-state probability density isosurfaces of the CDV Fokker–Planck equation with multiplicative and additive noise: $\sigma_i^M = 0.3$ and $\sigma_i^A = 0.3$ ($i = 1, 2, 3$); $a = 1$, $b = 1$, $C = 0.2$, $x_1^* = 4.19$, $\beta = 2.55$. Isosurface values from upper left to lower right: 0.75, 1.25, 1.75, 2.25.

structure of the probability density changes as a function of the multiplicative noise level. The system shows a nearly monomodal low-index behavior for weak multiplicative noise. Increasing the noise level to intermediate intensities, the system becomes bimodal. Strong multiplicative noise squeezes the system into the zonal high-index state. Thus, the system undergoes a noise-induced transition (Horsthemke and Lefever 1984). It is important to note, that for the CDV Fokker–Planck equation there is no significant difference between the Stratonovich and the Itô interpretation. Numerical experiments show that both stochastic calculi show the same noise-induced regime transition. This qualitative equivalence of both stochastic calculi is due to the linearity of the multiplicative noise terms. In this linear case, the contribution of the stochastic drift is negligible for small multiplicative noise amplitudes.

b. Numerical solutions of the stochastic CDV model and mechanism of the noise-induced transition

To verify and interpret the results of the Fokker–Planck equation, numerical integrations of the stochastic

CDV model (6) using the Stratonovich interpretation are performed. The SDE is numerically solved by the stochastic Euler scheme (Rümelin 1982; Kloeden and Platen 1992). For a time-discrete approximation the Gaussian white noise η_i does have the standard deviation σ , because the continuous restriction $\langle \eta(t)\eta(t') \rangle = \sigma^2 \delta(t - t')$ cannot be implemented numerically. Thus, for discrete time steps the Gaussian white noise fulfills

$$\langle \eta_i \rangle = 0, \quad \langle \eta_i \eta_{i'} \rangle = \sigma^2 \delta_{ii'}, \quad (8)$$

where $\delta_{ii'}$ denotes the Kronecker delta. The parameters used for the subsequent experiments are the same as in the previous section. Using a time step of 0.01 the stochastic CDV model is integrated for 10 000 nondimensional units, which equals a dimensional interval of about 106 years. Note that a single experiment is only one finite realization of a stochastic process. The stationary solution of the corresponding Fokker–Planck equation, however, yields the probability density function for an infinite number of stochastic realizations. Time series of the x_1 component of the stochastic CDV model using multiplicative noise with standard deviations $\sigma_i^M = 0.1, 0.2, 0.3$, and 0.4 are shown in Fig. 6.

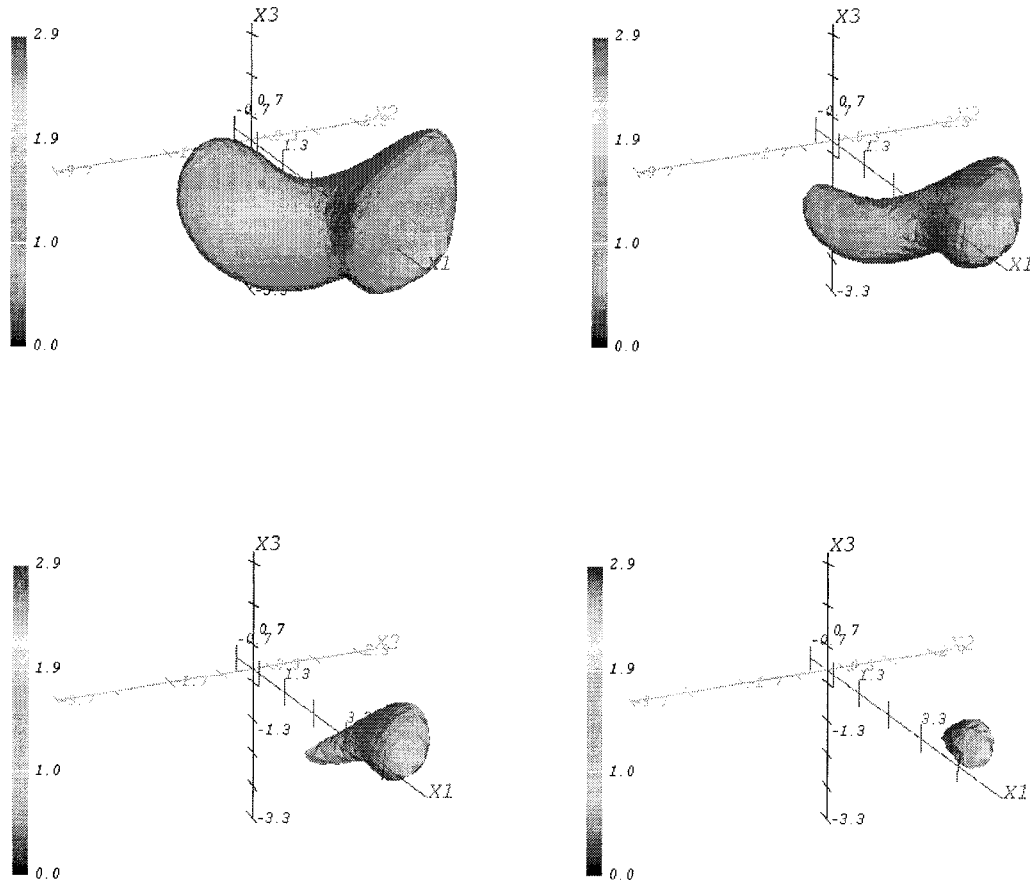


FIG. 5. Steady-state probability density isosurfaces of the CDV Fokker-Planck equation with multiplicative and additive noise: $\sigma_i^M = 0.4$ and $\sigma_i^A = 0.3$ ($i = 1, 2, 3$); $a = 1$, $b = 1$, $C = 0.2$, $x_1^* = 4.19$, $\beta = 2.55$. Isosurface values from upper left to lower right: 0.75, 1.25, 1.75, 2.25.

For convenience, only intervals of 1000 nondimensional units are shown. The corresponding histograms of the entire time series consisting of 10 000 units are shown in Fig. 7.

For $\sigma_i^M = 0.1$ the trajectory of the system remains near the blocked low-index equilibrium E_3 with $x_1 = 0.94$ for the entire integration (Fig. 6a). The corresponding histogram (Fig. 7a) illustrates the monomodal behavior. If the standard deviation of the multiplicative noise is enhanced to $\sigma_i^M = 0.2$, the system temporarily attains the zonal high-index state E_1 with $x_1 = 3.91$ (Fig. 6b). Note that the trajectories variance is somewhat lower in the zonal state compared to the blocked state. The bimodality of the system is visualized by the corresponding histogram (Fig. 7b), whereby the probability of the blocked state is somewhat higher than the probability of the zonal state. Further enhancement of the standard deviation ($\sigma_i^M = 0.3$) changes the bimodal behavior such that the system's trajectory visits the neighborhood of the zonal state E_1 (Fig. 6c) more often. Furthermore, the variance of the blocked state is enhanced, whereas the variance of the zonal state approximately remains unchanged. Therefore, the corresponding his-

togram (Fig. 7c) retains the bimodality, but reveals that the zonal state becomes the most probable regime. Finally, if the standard deviation of the multiplicative noise is enhanced to $\sigma_i^M = 0.4$, the variance of the blocked state increases noticeably (Fig. 6d). Nevertheless, the characteristic of the zonal regime remains nearly unchanged. The histogram illustrates that the bimodality vanished in favor of the zonal high-index state (Fig. 7d).

In summarizing, one observes that the stochastic CDV model (6) shows the same noise-induced transition as the corresponding Fokker-Planck equation (7). Nevertheless, a realization of a stochastic process reveals the mechanism of a noise-induced transition. As described previously, one observes (Fig. 6) that the variance of the trajectory in the blocked state increases as the multiplicative noise level is enhanced, whereas the trajectories variance in the zonal state remains nearly unchanged. This behavior can be explained by the mechanism of a noise-induced transition. A schematic illustration is presented in Fig. 8. For convenience, only a one-dimensional system with two stable equilibria, E_1 and E_3 , is considered. It is important to note that the

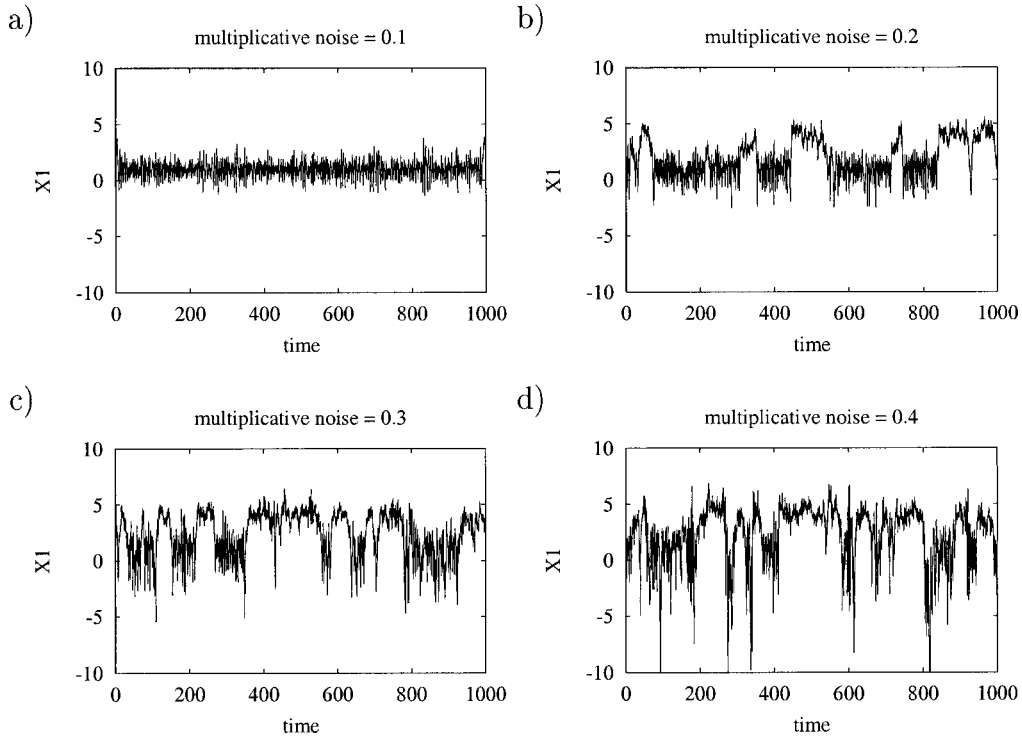


FIG. 6. Time series of the x_1 component of the stochastic CDV model with additive and multiplicative noise: $a = 1$, $b = 1$, $C = 0.2$, $x_1^* = 4.19$, $\beta = 2.55$, $\sigma_i^A = 0.3$ ($i = 1, 2, 3$). (a) $\sigma_i^M = 0.1$, (b) $\sigma_i^M = 0.2$, (c) $\sigma_i^M = 0.3$, (d) $\sigma_i^M = 0.4$. Note the noise-induced regime transition.

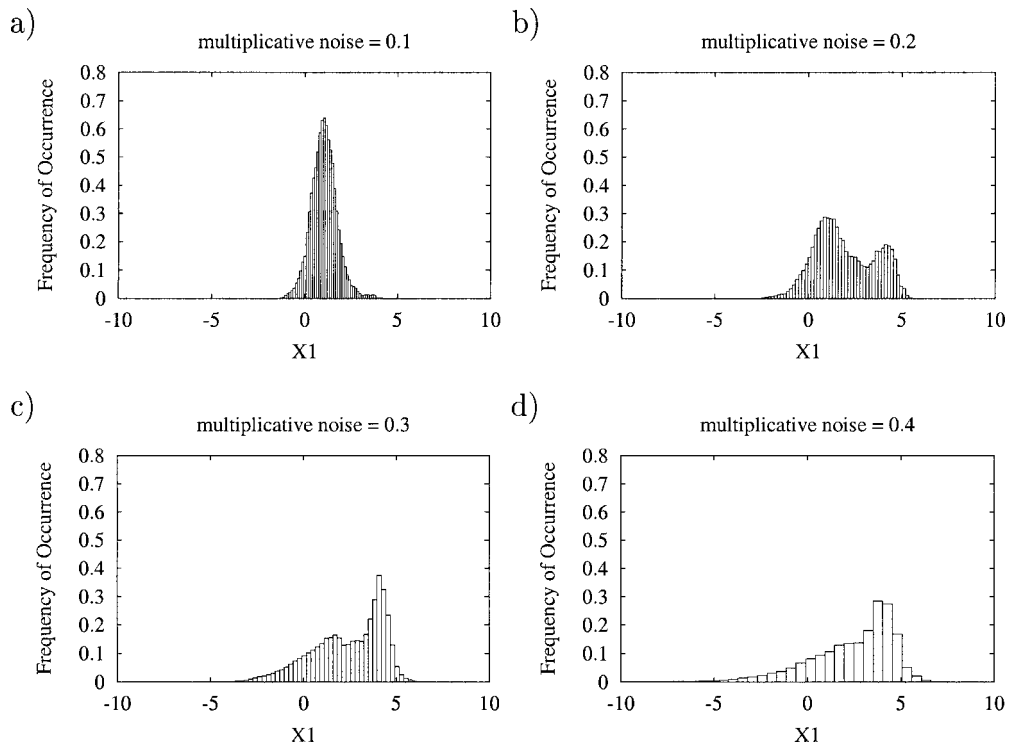


FIG. 7. Normalized histograms of the x_1 component of the stochastic CDV model with additive and multiplicative noise: $a = 1$, $b = 1$, $C = 0.2$, $x_1^* = 4.19$, $\beta = 2.55$, $\sigma_i^A = 0.3$ ($i = 1, 2, 3$). (a) $\sigma_i^M = 0.1$, (b) $\sigma_i^M = 0.2$, (c) $\sigma_i^M = 0.3$, (d) $\sigma_i^M = 0.4$. Note the noise-induced regime transition.

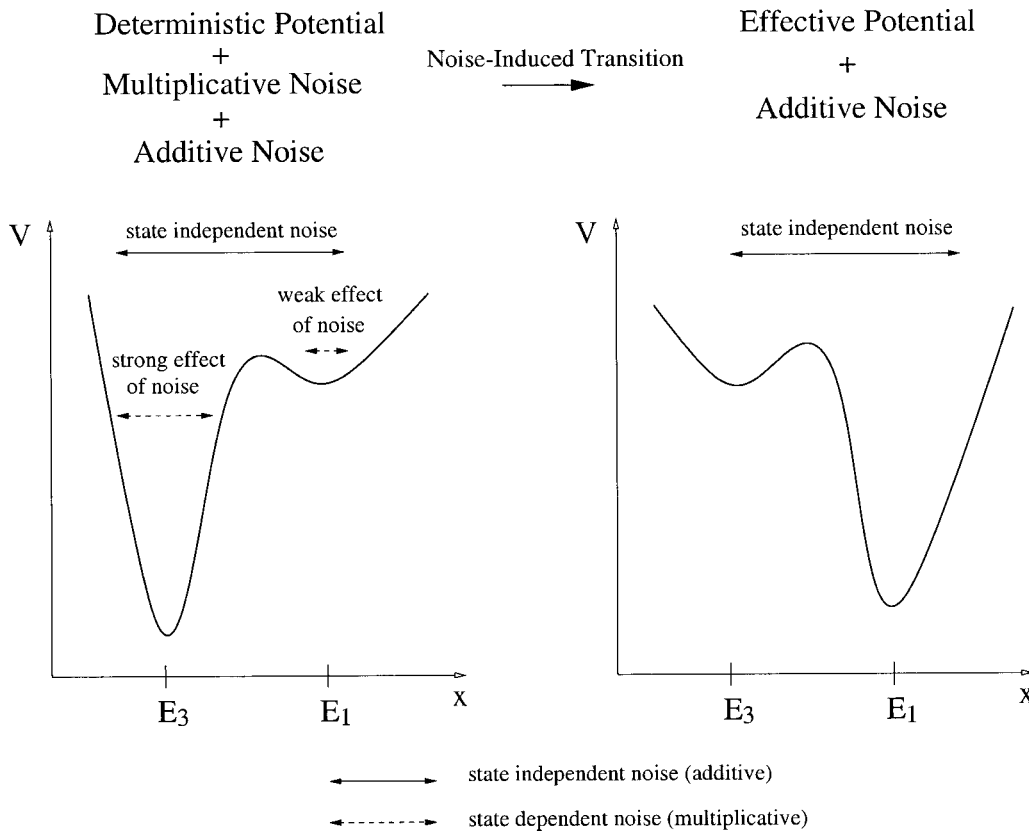


FIG. 8. Schematic mechanism of the noise-induced transition. The illustration shows the mechanism of the noise-induced transition *at the moment* the multiplicative noise is thought to be switched on.

illustration shows the mechanism of the noise-induced transition *at the moment* the multiplicative noise is thought to be switched on. The structure of the deterministic potential illustrates the dynamics and the stability properties of the system under consideration. With state independent, that is, additive, noise the stable state E_3 is the most probable regime, illustrated by the deep potential well. In contrast to E_3 , the other stable state E_1 is rarely attained by additive stochastic perturbations. The situation changes as soon as the system is perturbed by multiplicative noise. In this case the effect of the multiplicative noise depends on the state of the system. If, for example, the effect of the multiplicative noise is weaker in the neighborhood of equilibrium E_1 than in the neighborhood of E_3 , the dynamics of the stochastic system changes substantially. Such a situation occurs if the multiplicative stochastic term obeys $\dot{x} = \dots - \eta^M(x - x^*) + \eta^A$, with $x^* \approx E_1$. Then, the probability that the system's trajectory is found near E_1 increases as the amplitude of the multiplicative stochastic component is enhanced. Because of the larger amplitudes of the multiplicative noise in the neighborhood of E_3 , as compared to the neighborhood of E_1 , the system's trajectory is mainly found in the vicinity of E_1 . Furthermore, because the amplitudes of the stochastic perturbations are small in the vicinity of E_1 , the trajectory remains there for a

long time. That is, the probability of the two regimes is a function of the multiplicative noise level. The overall structure of the original deterministic potential changes due to the effect of the multiplicative noise and becomes an altered effective potential. This one-dimensional mechanism of a noise-induced transition can be extended to three dimensions, to explain the observed behavior of the stochastic CDV model with multiplicative noise.

Note that in *each* of the three dimensions the variance of the multiplicative noise term acts to push the system away from the low-index state, and gets weaker when the system is near the high-index state. In particular, the term $\dot{x}_1 = \dots - \eta_1^M(x_1 - x_1^*)$ steers the system toward x_1^* , as described above. Nevertheless, even the multiplicative noise terms in the remaining two dimensions $\dot{x}_2 = \dots - \eta_2^M x_2$ and $\dot{x}_3 = \dots - \eta_3^M x_3$ steer the system toward lower absolute values of x_2 and x_3 , and therefore nearer to the high-index state. Remember that x_2 and x_3 of the high-index state $E_1 = (3.91, 0.74, -0.06)$ have smaller absolute values than the corresponding coordinates of the low-index state $E_3 = (0.94, -1.06, -0.65)$. Numerical experiments with multiplicative noise only in the forcing term support this conjecture; in this particular case the multiplicative noise has to be

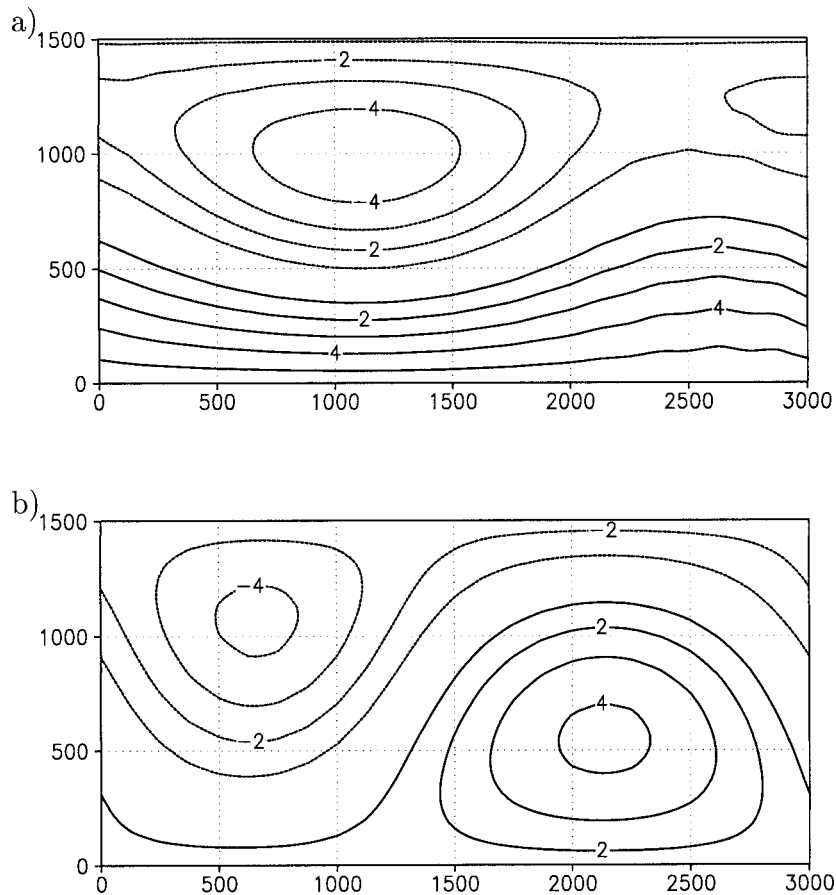


FIG. 9. Dimensional streamfunction patterns ($10^6 \text{ m}^2 \text{ s}^{-1}$) for the two stable equilibria of the gridpoint model: (a) zonal high-index state, (b) blocked low-index state. The axes are horizontal distances in kilometers.

very much stronger to force the noise-induced transition toward the zonal high-index state.

c. Qualitative comparison with a gridpoint model

This section will confirm that the noise-induced transition found for the low-order spectral model also occurs, in a qualitative sense, in a numerical integration of a gridpoint model with many more degrees of freedom. Charney and DeVore (1979) and Yoden (1985b) show that the existence of multiple equilibria is not an artifact of the low-order model. The corresponding gridpoint, respectively high-order spectral model shows two stable equilibria as well.

The dimensional quasigeostrophic vorticity equation (1) with topography and forcing (2) and parameters summarized in Table 1 is numerically solved by standard finite differences in space and time. Space differencing is performed by space-centered approximations. In particular, the nonlinear Jacobian is approximated by the Arakawa scheme. Time differencing is performed by the third-order Adams–Bashforth scheme. The Helmholtz equation appearing at each time step is solved by

cyclic reduction. The spatial resolution is $\Delta x = 120 \text{ km}$ in the zonal, and $\Delta y = 60 \text{ km}$ in the meridional direction. Thus, the channel has 25×25 grid points. The time step is 1 h. The streamfunction is saved once a day. For all further purposes these daily data are used to visualize the stochastically induced variability. The additive white noise is just an additional term in (1). The multiplicative noise is implemented by stochastically perturbing the Ekman layer depth D_E , that is, the damping of the flow. Thus, D_E stochastically fluctuates around the mean value \bar{D}_E : $D_E = \bar{D}_E + \eta(t)$.

Indeed, the deterministic gridpoint model has two stable equilibria for the used parameter values. The corresponding streamfunction patterns are shown in Fig. 9. The first stable equilibrium in Fig. 9a consists of a zonal high-index regime, whereas the second stable state in Fig. 9b shows a blocked low-index flow. These two stationary solutions resemble the two stable equilibria of the deterministic low-order CDV model (see Fig. 1). Nevertheless, the zonal high-index state of the gridpoint model has a different structure compared to the low-order model. In particular, the high-index state of the gridpoint model does not have the spatial symmetry with

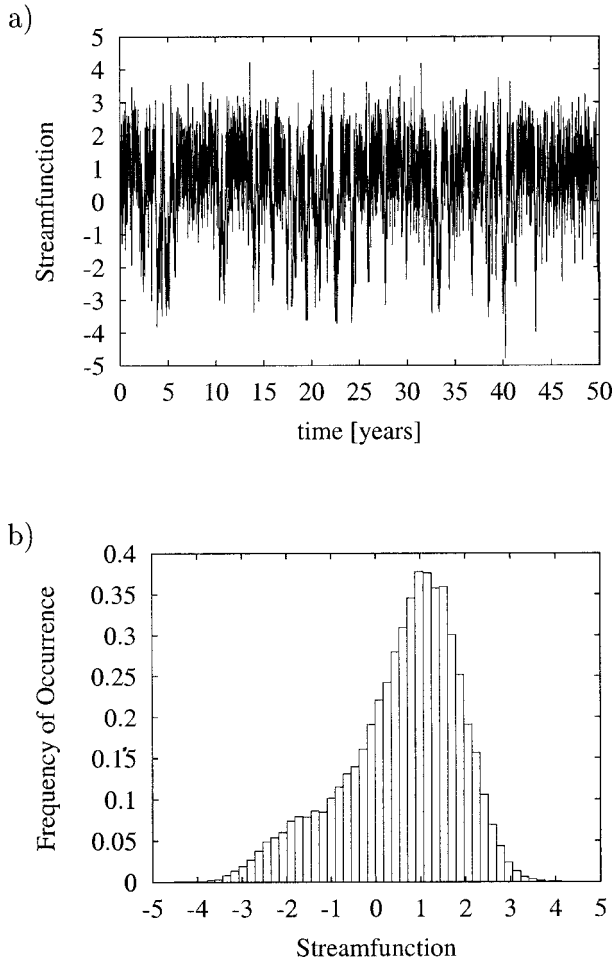


FIG. 10. (a) Time series of the dimensional streamfunction ($10^6 \text{ m}^2 \text{ s}^{-1}$) in the center of the channel ($x = 1500 \text{ km}$, $y = 750 \text{ km}$) for the gridpoint model with additive noise only. Positive streamfunction values characterize the blocked state; negative streamfunction values characterize the zonal state (see Fig. 9). (b) The corresponding normalized histogram.

respect to the transformation $\psi(x, y) \rightarrow \psi(x + \pi/2, \pi - y)$; see Yoden (1985b) for the symmetry properties of the CDV vorticity equation. Notwithstanding that, the gridpoint model has two stable equilibria which at least resemble a zonal high-index regime and a blocked low-index flow.

With additive noise both the stochastic low-order CDV model and the stochastic gridpoint model show qualitatively similar results. A 50-yr-long time series of the dimensional streamfunction in the center of the channel ($x = 1500 \text{ km}$, $y = 750 \text{ km}$) is shown in Fig. 10a. Positive streamfunction values characterize the blocked state, negative streamfunction values characterize the zonal state (see Fig. 9). The corresponding histogram is shown in Fig. 10b. It is perceivable that in the additively perturbed gridpoint model the blocked low-index flow is the most probable regime. The zonal high-index flow, however, is of secondary importance.

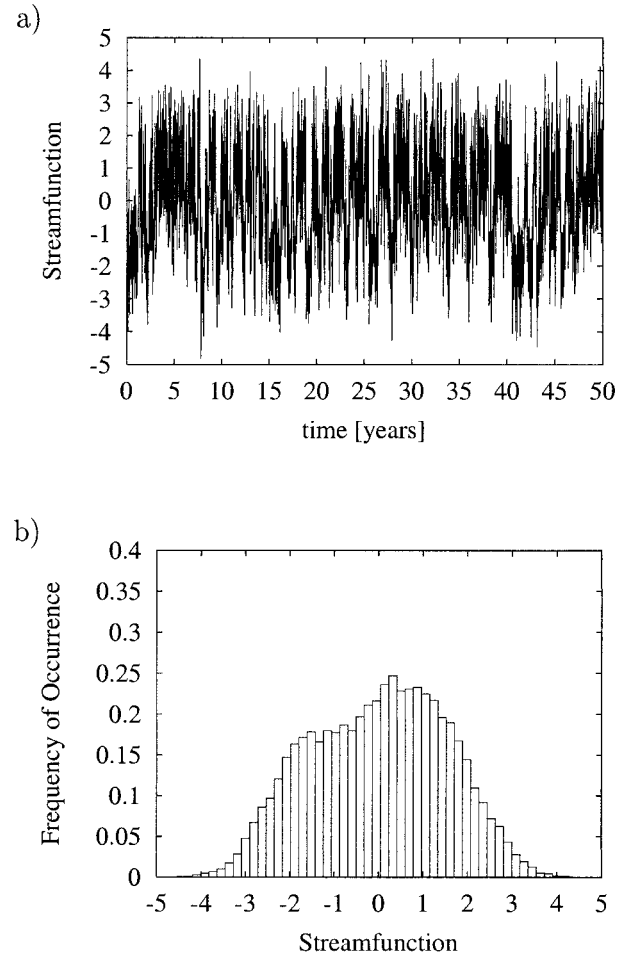


FIG. 11. (a) Time series of the dimensional streamfunction ($10^6 \text{ m}^2 \text{ s}^{-1}$) in the center of the channel ($x = 1500 \text{ km}$, $y = 750 \text{ km}$) for the gridpoint model with additive and multiplicative noise. Positive streamfunction values characterize the blocked state; negative streamfunction values characterize the zonal state (see Fig. 9). (b) The corresponding normalized histogram.

That is, the behavior of the additively perturbed stochastic CDV model is not an artifact of the low-order spectral truncation, but is qualitatively found in the stochastic high-order gridpoint model as well.

The qualitative behavior of the stochastic gridpoint model changes as soon as multiplicative noise is added in addition to additive noise. With additional multiplicative noise even the high-order gridpoint model shows a noise-induced transition. That is, with multiplicative noise the probability that the system attains the zonal regime increases significantly. This behavior is clearly seen in Fig. 11. As before, in Fig. 11a, a 50-yr-long time series of the dimensional streamfunction in the center of the channel ($x = 1500 \text{ km}$, $y = 750 \text{ km}$) is shown. The corresponding histogram is shown in Fig. 11b. For the presented results the standard deviation of the multiplicative noise that perturbs the Ekman layer depth is 300 m. Sensitivity experiments show that the

observed phenomenon is indeed a pure noise-induced transition: Similar results cannot be obtained with additive noise only. Nevertheless, it is not possible to raise the probability of the zonal state beyond the presented bimodal distribution; for higher multiplicative noise levels the gridpoint model is not numerically stable any more.

In summarizing, the noise-induced transition observed within the framework of the low-order stochastic CDV model is at least qualitatively confirmed to some extent by numerical stochastic integrations of the corresponding gridpoint model with many more degrees of freedom than the low-order model. Thus, the noise-induced transition is not an artifact of the low-order model.

4. Summary and discussion

The concepts of multiplicative stochastic perturbations and noise-induced transitions are applied to a quasigeostrophic β -plane model of barotropic flow over topography. The spectral three-component low-order representation of this configuration yields the CDV model. In addition to an additive stochastic term the externally prescribed damping of the system is allowed to scatter around a mean value. This leads to a multiplicative stochastic forcing. The Fokker–Planck equation and the stochastic differential equation of the stochastic low-order CDV model are solved numerically. It is found that the behavior of the model changes as a function of the multiplicative noise level. The effect of multiplicative noise is not simply a smoothing of the probability density function, as it would be for pure additive noise. Rather, multiplicative noise leads to the high-index state being favored over the low-index state. In particular, the system shows a nearly monomodal low-index behavior for weak multiplicative noise. Increasing the noise level to intermediate intensities, the system becomes bimodal. Strong multiplicative noise squeezes the system into the zonal high-index state. The concept of noise-induced transitions explains this qualitative behavior. Furthermore, the relationship to the stochastically perturbed high-order gridpoint model is studied. It is found that the noise-induced transition observed within the framework of the low-order stochastic CDV model is at least qualitatively confirmed by numerical integrations of the corresponding gridpoint model with many more degrees of freedom than the low-order model. Therefore, the noise-induced transition is not an artifact of the low-order model. Thus, the results of the present paper illustrate the phenomenon of a noise-induced transition and, furthermore, show that multiplicative noise can have a crucial effect on the qualitative behavior of the barotropic quasigeostrophic equation.

A comparable result for the qualitative behavior of the North Atlantic thermohaline circulation is presented by Timmermann and Lohmann (2000). The authors use a simplified box ocean model to study the influence of multiplicative short-term climate variability on the sta-

bility and long-term dynamics of the thermohaline circulation. As a result the behavior of the thermohaline circulation becomes a function of the noise level. Thus, the system undergoes a noise-induced transition.

In general, these findings illustrate that the qualitative behavior of simplified climate models can be significantly altered by the stochastic representation of external parameters, that is, by the use of multiplicative noise. Another issue raised is the question of how reliable deterministic bifurcation or stability analysis is. In particular, it is questionable to what extent the analysis of a deterministic system reveals the behavior of the corresponding stochastic systems. The probability density in the phase space of a nonlinear stochastic system can be entirely different from the probability density of the deterministic system.

Although the models used in the present paper are very simple, it is expected that the use of multiplicative noise and the concept of noise-induced transitions is useful to understand the behavior of large-scale atmospheric dynamics. It deserves further research to understand the influence of multiplicative noise in more complex models.

Acknowledgments. I thank Klaus Fraedrich, Frank Lunkeit, Christoph Raible, and Cécile Penland for helpful discussions and support. I thank Timothy DelSole and one anonymous reviewer for valuable comments that led to improvements of the original manuscript. This work was supported by the Deutsche Forschungsgemeinschaft within Sonderforschungsbereich 512.

APPENDIX

Derivation of the Low-Order Spectral Model

In this appendix the low-order spectral model used in the present paper is derived. The scaling is identical to DeSwart and Grasman (1987). See section 2 for a more detailed description of the underlying dimensional model.

With the rigid-lid approximation ($\gamma^2 = 0$), the characteristic height H , the timescale σ^{-1} , the horizontal length scale k^{-1} , and the characteristic amplitude of the topography h_0 , the nondimensional quasigeostrophic vorticity equation reads

$$\begin{aligned} \frac{\partial}{\partial t} \nabla^2 \psi + J(\psi, \nabla^2 \psi) + \bar{\gamma} J(\psi, h) + \bar{\beta} \frac{\partial \psi}{\partial x} \\ = -\bar{C} \nabla^2 (\psi - \psi^*), \end{aligned} \quad (\text{A1})$$

with the parameters

$$\bar{\gamma} = \frac{f_0 h_0}{\sigma H}, \quad \bar{\beta} = \frac{\beta}{\sigma k}, \quad \bar{C} = \frac{f_0 D_E}{2\sigma H}. \quad (\text{A2})$$

By letting $k = 2\pi/L_x$, the nondimensional domain of the channel is $0 \leq x \leq 2\pi$ and $0 \leq y \leq \pi b$, with $b = 2L_y/L_x$.

The low-order spectral model is developed by expanding the nondimensional streamfunction ψ in three orthonormal modes, $\psi = \psi_1 + \psi_2 + \psi_3$. These modes are

$$\begin{aligned}\psi_1 &= \bar{\psi}_1 \phi_1 = \bar{\psi}_1 \sqrt{2} \cos\left(\frac{y}{b}\right) \\ \psi_2 &= \bar{\psi}_2 \phi_2 = \bar{\psi}_2 2 \cos(x) \sin\left(\frac{y}{b}\right) \\ \psi_3 &= \bar{\psi}_3 \phi_3 = \bar{\psi}_3 2 \sin(x) \sin\left(\frac{y}{b}\right).\end{aligned}\quad (\text{A3})$$

The nondimensional topography and forcing read

$$\begin{aligned}h(x, y) &= \frac{1}{2} \phi_2 = \cos(x) \sin\left(\frac{y}{b}\right), \\ \psi^* &= \psi_0^* \phi_1 + \psi_0^* \sqrt{2} \cos\left(\frac{y}{b}\right).\end{aligned}\quad (\text{A4})$$

Next (A3) and (A4) are inserted into the quasigeostrophic vorticity equation (A1). Utilizing the orthonormality of the eigenfunctions ϕ_i , putting $x_i = \bar{\psi}_i/b$, $\sigma = f_0 h_0/H$, and defining the new time $\bar{t} = (4\sqrt{2}/3\pi)t$, the low-order model becomes

$$\begin{aligned}\dot{x}_1 &= bx_3 - C(x_1 - x_1^*) \\ \dot{x}_2 &= -ab\left(x_1 - \frac{1}{2}\beta\right)x_3 - Cx_2 \\ \dot{x}_3 &= ab\left(x_1 - \frac{1}{2}\beta\right)x_2 - \frac{1}{2}ax_1 - Cx_3,\end{aligned}\quad (\text{A5})$$

with

$$\begin{aligned}a &= \frac{2b}{1+b^2}, \quad \beta = \frac{3\pi}{4\sqrt{2}}\bar{\beta}, \quad C = \frac{3\pi}{4\sqrt{2}}\bar{C}, \\ x_1^* &= \frac{Uk}{\sigma}.\end{aligned}\quad (\text{A6})$$

The velocity scale U is connected with the dimensional amplitude of the streamfunction forcing ψ_0^* through the relation $\psi_0^* = Ub\sqrt{2}/k$.

REFERENCES

- Benzi, R., A. R. Hansen, and A. Sutera, 1984: On stochastic perturbation of simple blocking models. *Quart. J. Roy. Meteor. Soc.*, **110**, 393–409.
- Chang, J. S., and G. Cooper, 1970: A practical difference scheme for Fokker–Planck equations. *J. Comput. Phys.*, **6**, 1–16.
- Charney, J. G., and J. G. DeVore, 1979: Multiple flow equilibria in the atmosphere and blocking. *J. Atmos. Sci.*, **36**, 1205–1216.
- Corti, S., F. Molteni, and T. N. Palmer, 1999: Signature of recent climate change in frequencies of natural atmospheric circulation regimes. *Nature*, **29**, 799–802.
- DeSwart, H. E., 1988: Low-order spectral models of the atmospheric circulation: A survey. *Acta Appl. Math.*, **11**, 49–96.
- , and J. Grasman, 1987: Effect of stochastic perturbations on a low-order spectral model of the atmospheric circulation. *Tellus*, **39A**, 10–24.
- Dethloff, K., A. Weisheimer, A. Rinke, D. Handorf, M. V. Kurgansky, W. Jansen, P. Maaß, and P. Hupfer, 1998: Climate variability in a nonlinear atmosphere-like dynamical system. *J. Geophys. Res.*, **103**, 25 957–25 966.
- Egger, J., 1981: Stochastically driven large-scale circulations with multiple equilibria. *J. Atmos. Sci.*, **38**, 2606–2618.
- Gardiner, C. W., 1985: *Handbook of Stochastic Methods for Physics, Chemistry and the Natural Science*. 2d ed. Springer-Verlag, 442 pp.
- Horsthemke, W., and R. Lefever, 1984: *Noise-Induced Transitions: Theory and Applications in Physics, Chemistry, and Biology*. Springer-Verlag, 318 pp.
- Kloeden, P., and E. Platen, 1992: *Numerical Solution of Stochastic Differential Equations*. Springer-Verlag, 632 pp.
- Kurgansky, M. V., K. Dethloff, I. A. Pisnichenko, H. Gernandt, F.-M. Chmielewski, and W. Jansen, 1996: Long-term climate variability in a simple nonlinear atmospheric model. *J. Geophys. Res.*, **101**, 4299–4314.
- Landa, P. S., and P. V. E. McClintock, 2000: Changes in the dynamical behavior of nonlinear systems induced by noise. *Phys. Rep.*, **323**, 1–80.
- Legras, B., and M. Ghil, 1985: Persistent anomalies, blocking and variations in atmospheric predictability. *J. Atmos. Sci.*, **42**, 433–471.
- Majda, A. J., I. Timofeyev, and E. Vanden Eijnden, 1999: Models for stochastic climate prediction. *Proc. Nat. Acad. Sci. U.S.A.*, **96**, 14 687–14 691.
- Pandolfo, L., 1993: Observational aspects of the low-frequency intraseasonal variability of the atmosphere in middle latitudes. *Advances in Geophysics*, Vol. 34, Academic Press, 93–174.
- Park, B. T., and V. Petrosian, 1996: Fokker–Planck equations of stochastic acceleration: A study of numerical methods. *Astrophys. J., Suppl. Ser.*, **103**, 255–267.
- Pedlosky, J., 1987: *Geophysical Fluid Dynamics*. 2d ed. Springer Verlag, 710 pp.
- Press, W. H., S. A. Teukolsky, W. T. Vetterling, and B. P. Flannery, 1992: *Numerical Recipes in Fortran, The Art of Scientific Computing*. Cambridge University Press, 963 pp.
- Rümelin, W., 1982: Numerical treatment of stochastic differential equations. *SIAM J. Numer. Anal.*, **19**, 604–613.
- Sardeshmukh, P., C. Penland, and M. Newman, 2001: Rossby waves in a fluctuating medium. *Stochastic Climate Models*, P. Imkeller and J.-S. von Storch, Eds., vol. 49, *Progress in Probability*, Birkhäuser Verlag.
- Timmermann, A., and G. Lohmann, 2000: Noise-induced transitions in a simplified model of the thermohaline circulation. *J. Phys. Oceanogr.*, **30**, 1891–1900.
- Tung, K. K., and A. J. Rosenthal, 1985: Theories of multiple equilibria—A critical reexamination. Part I: Barotropic models. *J. Atmos. Sci.*, **42**, 2804–2819.
- Yoden, S., 1985a: Bifurcation properties of a quasi-geostrophic, barotropic, low-order model with topography. *J. Meteor. Soc. Japan*, **63**, 535–546.
- , 1985b: Multiple stable states of quasi-geostrophic barotropic flow over sinusoidal topography. *J. Meteor. Soc. Japan*, **63**, 1031–1044.